Highly Emissive Pyrene-excimer Formation in Self-assembled Monolayer on Gold Surface and Photocurrent Generation from the Excimer

Mitsunobu Nakamura,* Norikazu Saito, Kaori Takayama,
Satoshi Kumamoto, and Kazushige Yamana*
Department of Materials Science and Chemistry, Graduate School of Engineering,
University of Hyogo, 2167 Shosha, Himeji 671-2201

(Received February 5, 2007; CL-070132; E-mail: mitunobu@eng.u-hyogo.ac.jp, yamana@eng.u-hyogo.ac.jp)

Strong pyrene excimer fluorescence is observed in the SAM derived from disulfide-functionalized bis-pyrene derivative on gold surface at the pyrene surface coverage similar to that exhibits only weak monomer fluorescence in the SAM derived from disulfide-functinalized monopyrene derivative. The pyrene excimer is less sensitive to the quenching by gold substrate than pyrene monomer excited state. The photocurrent generates from the excimer emissive SAM more effectively than the monomer emissive SAM.

Pyrene excimer fluorescence has been widely used as a probe light in chemosensor,[1–5] biosensor,[6–10] or optical device,[11–14] because of its high quantum efficiency at visible wavelength region (>400 nm). In addition, it is less subject to quenching by electron donors or acceptors than pyrene monomer fluorescence.[15] Pyrene excimer formation has also been studied in self-assembled monolayers (SAMs) on metal surface.[16–21] In densely packed pyrene-monolayers, however, the excimer emission usually suffers from self-quenching due to the chromophore aggregation.

We have been interested in pyrene-excimer-forming SAMs in relation to development of a signal transduction element in biosensors. An electronic signal could be obtained though photo-electrochemical conversion in the SAMs. However, little has been known about the photoelectrochemical properties of pyrene-excimer-forming SAM. In this communication, we describe that bis-pyrene-functionalized SAM with controlled assembly on gold surface exhibits strong excimer emission. The pyrene-excimer-forming SAM can generate photocurrent more efficiently when compared to the pyrene monomer fluorescence emitting SAM.

The pyrene derivatives (**P*n***s) employed in this work are illustrated in Figure 1. The fluorescence spectrum of **P1** in dioxane solution (5×10^{-6} M) shows only pyrene monomer fluorescence with emission maximum at 377 nm. In contrast, the fluorescence spectrum of **P2** in dioxane (5×10^{-6} M) shows excimer fluorescence around 480 nm as major fluorescence (Figure S1 in Supporting Information). For controlled assembly of **P*n*** on gold surface, we used 2,2′-ditiodiethanol (**DTE**) as a coadsorbent. The SAM derived from **P*n*** on gold electrode (**Au–P*n***) was prepared by immersing Au(111)/slide glass for 24 h into the dioxane solution of **P*n*** (5 mM) containing 5 mM of **DTE**. The surface coverage of pyrene chromophore on **Au–P*n***s were estimated to be 1.31×10^{-10} mol/cm^2 for **Au–P1** and 1.38×10^{-10} mol/cm^2 for **Au–P2** by means of the method reported by Blanchard and co-workers.[22,23]

Figure 2 shows the surface reflectance fluorescence and excitation spectra of **Au–P*n***s. The typical pyrene monomer fluorescence is observed for **Au–P1** with maximums at 378 and 400 nm. The fluorescence spectrum of **Au–P2** exhibits the broad emission band around 460 nm. While the fluorescence quantum yield of **P2** is about 1.5 times higher than that of **P1** in dioxane, the fluorescence quantum yield for **Au–P2** seems to be more than 10 times higher than that for **Au–P1**. The excitation spectra of both SAMs show the spectral features characteristic of pyrene absorption with maximums at 331, 348 nm for **Au–P1** and 335, 352 nm for **Au–P2**. The agreement of the both excitation spectra in spectral features indicates that the origin of the fluorescence for **Au–P1** and **Au–P2** is pyrene chromophore. The broad emission band in the fluorescence spectrum for **Au–P2** is thus assignable to pyrene excimer fluorescence. Close examination of the excitation spectra reveals that the excimer formation may be due to the excitation of stacked pyrenes in ground state, because the excitation maximum of **Au–P2** shifts to lower energy than that of **Au–P1**.

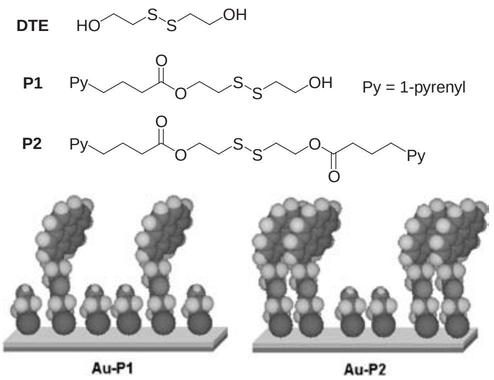

Figure 1. Structure of pyrene-containing self-assembled monolayers on gold (**Au–P*n***s).

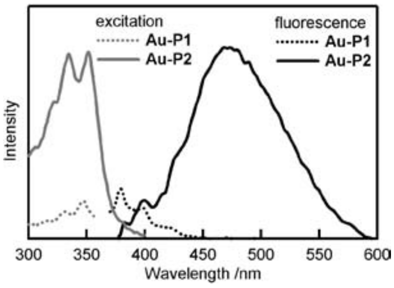

Figure 2. Surface reflectance fluorescence spectra ($\lambda_{ex} = 345$ nm) and excitation spectra of **Au–P*n***s. The excitation spectra were monitored at 378 nm for **Au–P1** and 465 nm for **Au–P2**.

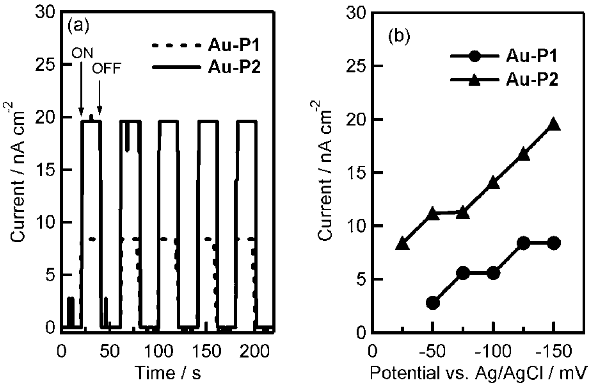

Figure 3. Panel (a): Photoelectrochemical responses of **Au–P*n*** systems at −150 mV of applied voltage. Panel (b): Photocurrent dependency on applied bias voltage applied to **Au–P*n*** systems. Photoirradiation was carried out in an argon-saturated aqueous Na_2SO_4 (50 mM) solution containing 50 mM methyl viologen.

Photoelectrochemical measurements were carried out in an argon-saturated aqueous Na_2SO_4 (50 mM) solution containing 50 mM methyl viologen (MV^{2+}) as an electron carrier. The SAM **Au–P*n*** was used as the working electrode, along with a platinum counter electrode and an Ag/AgCl reference electrode in a three-electrode system.[24] Figure 3a shows the photoelectrochemical responses of **Au–P*n***s. Photoirradiation of **Au–P1** and **Au–P2** at −150 mV of constant applied voltage causes immediate generation of a photocurrent of 8.4 and 19.4 nA/cm^2, respectively. The photocurrents go down instantly when the irradiation is terminated. The photocurrent efficiency for excimer emissive **Au–P2** is more than two times higher than that for monomer emissive **Au–P1**.

The photocurrent generations under the various applied bias voltages were also investigated to determine the direction of the current flow. The negative bias to the gold electrode increased the cathodic photocurrent and semilinear correlation between the bias voltage and the cathodic photocurrent is observed in the region of −25–−150 mV vs. Ag/AgCl upon photoirradiation (Figure 3b). These results are indicative that the photocurrent flows from the gold electrode to the counter electrode through the SAM of **P*n***. The action spectrum for the photocurrent generation from **Au–P2** is similar to that from **Au–P1** and resembles the fluorescence excitation spectra of the SAM of **P*n*** (Figure S2). Therefore, the pyrene is photoactive species, and the photocurrent is oxidative current of the pyrene.[25]

Based on the photocurrent generation behaviors and spectral observations of **Au–P*n***s, the mechanism of photocurrent generation is considered as follows. The photocurrent flows from the gold electrode to the Pt wire that is mediated by the pyrene grand state/excited state couple and MV^{2+} as an electron acceptor. Despite the similar surface coverage of **Au–P*n***s, **Au–P2** shows only the excimer fluorescence that is exceedingly stronger than the monomer fluorescence of **Au–P1**. As a result, the electron pumping from the ground state to the excited state is efficient in the excimer emitting **Au–P2**, leading to the strong photocurrent. The photocurrent from **Au–P2**, however, did not exceed more than 10 times that from **Au–P1**. This is probably due to that the electron transfer from the pyrene excimer to MV^{2+} may be less efficient than from the monomer excited state. Further studies are necessary to clarify this point.

In summary, the bis-pyrene-functionalized SAM with controlled assembly can form pyrene excimer with high fluorescence quantum yield. Photocurrent is generated from the excimer emissive SAM more effectively than the monomer emissive SAM. To our knowledge, this is the first photocurrent observation from pyrene excimer in metal-surfaced monolayer. The present findings would be useful for the design of oligonucleotides incorporating appropriate chromophores for efficient photocurrent generation as well as be encouraging for elucidating the photoelectrochemical properties of helically stacked pyrene array.[26]

This research was partly supported by a Grant-in-Aid for Scientific Research from JSPS (M.N.).

References and Notes

1 B. Schazmann, N. Alhashimy, D. Diamond, *J. Am. Chem. Soc.* **2006**, *128*, 8607.
2 H. Yuasa, N. Miyagawa, T. Izumi, M. Nakatani, M. Izumi, H. Hashimoto, *Org. Lett.* **2004**, *6*, 1489.
3 X. Zhang, W.-D. Woggon, *J. Am. Chem. Soc.* **2005**, *127*, 14138.
4 S. K. Kim, S. H. Lee, J. Y. Lee, J. Y. Lee, R. A. Bartsch, J. S. Kim, *J. Am. Chem. Soc.* **2004**, *126*, 16499.
5 Y. Nakahara, T. Kida, Y. Nakatsuji, M. Akashi, *J. Org. Chem.* **2004**, *69*, 4403.
6 K. Yamana, Y. Fukunaga, Y. Ohtani, S. Sato, M. Nakamrua, W. J. Kim, T. Akaike, A. Maruyama, *Chem. Commun.* **2005**, 2509.
7 K. Yamana, T. Iwai, Y. Ohtani, S. Sato, M. Nakamura, H. Nakano, *Bioconjugate Chem.* **2002**, *13*, 1266.
8 E. G. Novikov, N. V. Visser, V. G. Malevitskaia, J. W. Borst, A. van Hoek, A. J. W. G. Visser, *Langmuir* **2000**, *16*, 8749.
9 K. J. Oh, K. J. Cash, K. W. Plaxco, *J. Am. Chem. Soc.* **2006**, *128*, 14018.
10 A. Okamoto, T. Ichiba, I. Saito, *J. Am. Chem. Soc.* **2004**, *126*, 8364.
11 S. Oshita, A. Matsumoto, *Langmuir* **2006**, *22*, 1943.
12 R. Y. Lai, J. J. Fleming, B. L. Merner, R. J. Vermeij, G. J. Bodwell, A. J. Bard, *J. Phys. Chem. A* **2004**, *108*, 376.
13 R. J. Brea, M. E. Va'zquez, M. Mosquera, L. Castedo, J. R. Granja, *J. Am. Chem. Soc.* **2007**, *129*, 1653.
14 M. Endo, H. Wang, M. Fujitsuka, T. Majima, *Chem. Eur. J.* **2006**, *12*, 3735.
15 R. A. Caldwell, D. Creed, D. C. DeMarco, L. A. Melton, H. Ohta, P. H. Wine, *J. Am. Chem. Soc.* **1980**, *102*, 2369.
16 M. Dominska, P. Krysinski, G. J. Blanchard, *J. Phys. Chem. B* **2005**, *109*, 15822.
17 P. V. Kamat, S. Barazzouk, S. Hotchandani, *Angew. Chem., Int. Ed.* **2002**, *41*, 2764.
18 B. I. Ipe, K. G. Thomas, *J. Phys. Chem. B* **2004**, *108*, 13265.
19 M. Montalti, L. Prodi, N. Zaccheroni, G. Battistini, *Langmuir* **2004**, *20*, 7884.
20 B. I. Ipe, K. G. Thomas, S. Barazzouk, S. Hotchandani, P. V. Kamat, *J. Phys. Chem. B* **2002**, *106*, 18.
21 T. Wang, D. Zhang, W. Xu, J. Yang, R. Han, D. Zhu, *Langmuir* **2002**, *18*, 1840.
22 M. Mazur, G. J. Blanchard, *J. Phys. Chem. B* **2005**, *109*, 4076.
23 M. Dominska, K. Jackowska, P. Krysinski, G. J. Blanchard, *J. Phys. Chem. B* **2005**, *109*, 15812.
24 Photocurrent measurements were carried in a quartz cell equipped with the modified gold electrode. The quartz cell was irradiated through UV-D36A band pass filter by a Xe lamp. The light intensity at the substrate surface was 157 μW/cm^2.
25 E. Soto, J. C. MacDonald, C. G. F. Cooper, W. G. McGimpsey, *J. Am. Chem. Soc.* **2003**, *125*, 2838.
26 M. Nakamura, Y. Ohtoshi, K. Yamana, *Chem. Commun.* **2005**, 5163.

Published on the web (Advance View) March 29, 2007; doi:10.1246/cl.2007.602